Room Temperature Synthesis of an 8-connected Zr-based Metal–Organic Framework for Top-down Nanoparticle Encapsulation

Hyunho Noh,[†] Chung-Wei Kung,[†] Timur Islamogu,[†] Aaron W. Peters,[†] Yijun Liao,[†] Peng Li,[†] Sergio J. Garibay,[†] Xuan Zhang,[†] Matthew R. Destefano,[†] Joseph T. Hupp,[†] and Omar K. Farha[†‡]*

†Department of Chemistry, and ‡Department of Chemical and Biological Engineering, Northwestern University, 2145 Sheridan Road, Evanston, Illinois 60208, United States

‡Department of Chemistry, Faculty of Science, King Abdulaziz University, Jeddah 21589, Saudi Arabia

■ Supporting Information

Table of Contents

Materials

Chemicals used for H_4TBAPy linker synthesis, as reported previously,[1] which are 1,3,6,8-tetrabromopyrene, tetrakis(triphenylphosphine), 4-(methoxycarbonyl)phenyl)boronic acid, tripotassium phosphate, palladium(0), chloroform, methanol, potassium hydroxide, 1,4-dioxane, acetone, N,N-dimethylformamide, were purchased from Sigma Aldrich Chemicals Company, Inc. (Milwaukee, WI) and were used as received. Nitric acid and hydrochloric acid were purchased from Fisher Scientific (Chicago, IL) and used as received. All chemicals used for the synthesis of Zr_6 node capped with twelve benzoates, which are the 80% solution of zirconium butoxide ($Zr(OBu)_4$) in 1-butanol, 1-propanol, and benzoic acid, were purchased from Sigma Aldrich Chemicals and were used as received. Ethylene glycol and chloroplatinic acid hydrdate ($H_2PtCl_6 \bullet xH_2O$) used for the nanoparticle (NP) synthesis were purchased from Sigma Aldrich Chemicals and were used as received. Polyvinylpyrrolidone (PVP, MW ~ 40,000) was purchased from Fluka (Milwaukee, WI) and was used as received. *Cis*-stilbene used for the hydrogenation was purchased from Sigma Aldrich Chemicals and was used as received.

Physical Measurements and Instrumentation

Prior to any soprtion measurement, approximately 60 mg of a sample was dried at 120 °C for 12 h under high vacuum using a Masterprep (Micromeritics, Norcross, GA). N_2 isotherms of all samples except the composite after catalysis were measured at 77 K using Micromeritics Tristar II 3020. For the sample after catalysis, ASAP-2020 was instead used for the measurement. BET surface area was calculated from measurements at the range P/P_0 = 0.005–0.1 following the criteria described before.[2] Density function theory (DFT) calculations using a carbon slit-pore model with a N_2 kernel were used to obtain the pore size distribution. Volumetric surface area was derived using the density calculated from the crystal structure of **NU-901** as reported previously.[3]

Thermogravimetric analysis (TGA) was performed using a TA Instruments Q500 under a N_2 flow at a ramp rate of 10 °C/min from 25 to 600 °C.

Scanning electron microscopy (SEM) images were collected at Northwestern University's EPIC/NUANCE facility using a Hitachi SU8030 FE-SEM (Dallas, TX) microscope. OsO_4 (~9 nm) was used to coat the specimen prior to the imaging.

Transmission electron microscopy (TEM) images were collected at Northwestern University's EPIC/NUANCE facility using a Hitachi HT7700 TEM using a standard copper mesh sample holder.

For the inductively-coupled plasma optical emission spectroscopy (ICP-OES), all samples were decomposed in 1 mL aqua regia solution (i.e. 0.75 mL HCl and 0.25 mL HNO_3 mixture) in a 2–5 mL Biotage microwave vial (Uppsala, Sweden) and were heated at 140 °C for 10 min with stirring using a SPX microwave reactor (software version 2.3, build 6250). **Caution:** *Heating an aqua regia solution can cause rapid build-up of pressure within the microwave vial. All digestions should be conducted with constant monitoring of the internal pressure*. The resulting solution was diluted to ~10 mL by adding ultrapure deionized water, which was further used for the elemental analysis using Varian Vista-MDX model ICP-OES spectrometer (Varian, Walnut Creek, CA) with a CCD detector and Ar plasma that covers 175–785 nm range. Emissions at 265.945, 214.423, and 203.646 nm for Pt and 339.198, 343.823, and 327.305 nm for Zr were used to determine the wt % of the sample.

X-ray photoelectron spectra (XPS) were measured at Keck-II/NUANCE facility at NU using a Thermo Scientific ESCALAB 250 Xi (Al Kα radiation, 1486.6 eV). Prior to any measurement, an electron flood gun equipped with the spectrometer was used and all collected spectra were calibrated to C 1s = 284.8 eV.

Powder X-ray diffraction (PXRD) patterns were collected on a Rigaku Smartlab instrument (Tokyo, Japan) with a $2\theta = 0.05°$ step size and 2°/min scan rate over 2–20° range at 45 kV and 160 mA.

A Shimadzu UV-3600 was used for the diffuse reflectance UV-Vis measurements. Spectra were collected from 200 to 800 nm with the Harrick Praying Mantis diffuse reflectance accessory.

For ^{1}H NMR samples, ~600 μL of the reaction mixtures were filtered to remove the solids, of which 540 μL was mixed with 60 μL of d_6-DMSO. The resulting mixtures were mounted onto Agilent DD2 500 MHz NMR.

Diffuse reflectance infrared Fourier transform (DRIFT) spectra were collected with a Nicolet S4 7600 FT-IR spectrometer equipped with an MCT detector. Resolutions were set to 1 cm^{-1} and solid KBr was used for a background spectrum and for dilution of solid samples. An average of 64 scans are plotted in **Figure S4**.

Gas Chromatography-mass spectrometry studies were carried out using an Agilent GC (6890)-mass spectrometer (5973N mass selective detector) with a DB5 column and an EI ionization source. The GC method started with an initial temperature of 50 °C for an initial time of 2 mins, then ramped at a rate of 20 °C/min to a final temperature of 320 °C. The compounds were identified using the NIST library of spectra.

Synthesis and Characterization of Zr_6 Node

The Zr_6 node was synthesized according to the reported procedure[4] with slight modification. To 300 mL of 1-propanol, 15 mL of 80 wt % $Zr(OBu)_4$ in *n*-butanol and 100 g of benzoic acid were added. The solution was sonicated for 10–20 min. Note at this stage, not all benzoic acid is soluble. The mixture was further heated under reflux for overnight under stirring, which resulted in a clear solution. Excess 1-propanol was removed by heating under vacuum, leading to crystallization of a white solid product. The solid was extensively washed with 1-propanol and was dried under vacuum at room temperature (yield ~ 63 %).

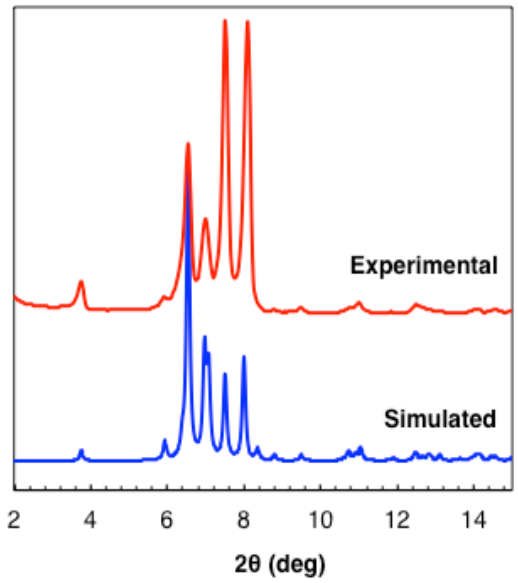

Figure S1. Experimental and simulated PXRD patterns of the Zr_6 node.

Pt/NU-901 Synthesis

Pt/NU-901 was synthesized analogously as to that reported previously.[5] Briefly, 10 mg of the freshly dried **NU-901-RT** and 1 mg of Pt NPs was dispersed in 20 mL of methanol. The suspension was sonicated and stirred for 2 hrs. The resulting solid was filtered through centrifugation, washed extensively with methanol three times, and was activated. The wt % loading, determined through an ICP-OES measurement analogous to that of **Pt@NU-901**, was determined to be 20.4 ± 0.2 wt %.

***Cis*-stilbene Hydrogenation Experimental Protocol**

The experimental protocol was adopted from that reported previously.[5] Briefly, 5 mg of the solid additives (or 2.7 mg for **Pt/NU-901** to keep the Pt wt % in the reaction mixture consistent) were added to 3.6 mL of ethyl acetate and 9.6 µL (20 eq. relative to Pt NPs) of *cis*-stilbene in a 25-mL Schlenk flask. The reaction mixture was freeze-pump-thawed prior to the introduction of 1 bar of H_2 gas and was left at room temperature for 1 h. The reaction was quenched using a dry ice/acetone bath and the substrate/product distribution was analyzed via ^{1}H NMR and GC-MS.

Characterization

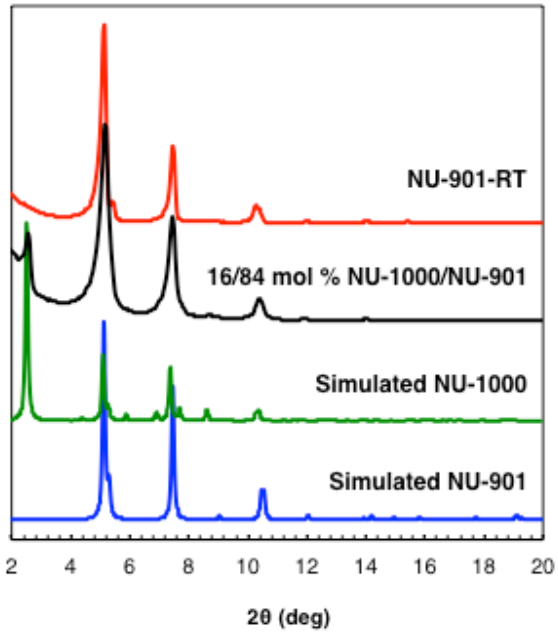

Figure S2. PXRD patterns of simulated **NU-901,** simulated **NU-1000,** physical mixture of 16/84 mol % **NU-1000**/**NU-901,** and **NU-901-RT**.

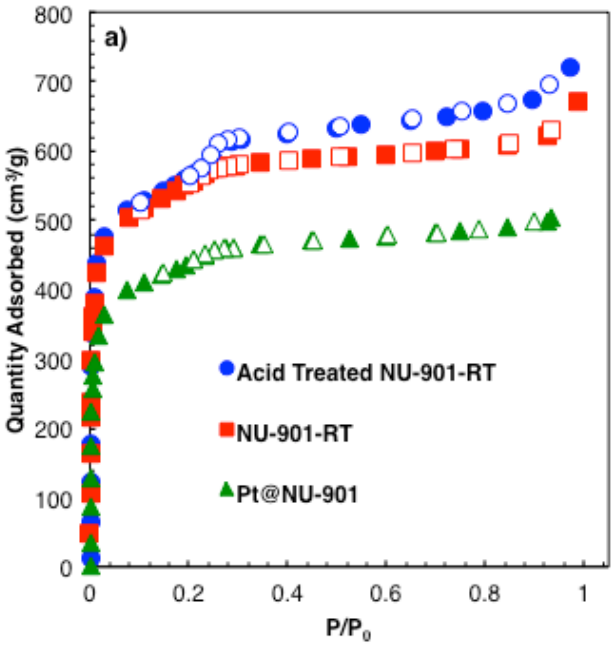

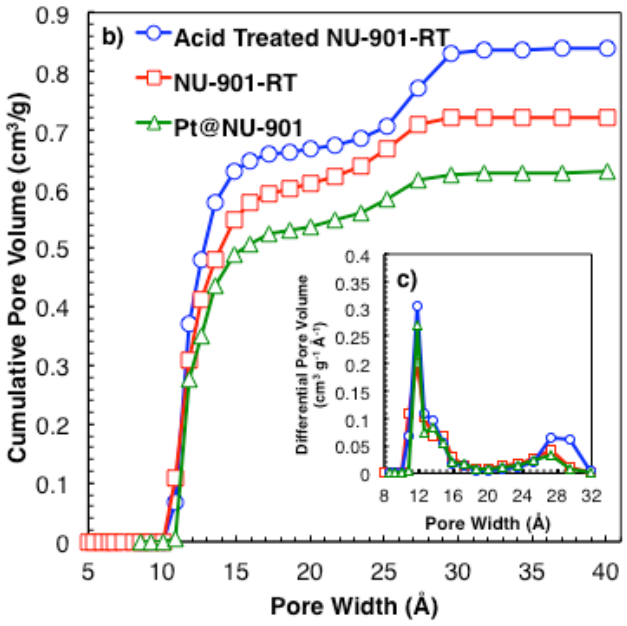

Figure S3. a) N_2 isotherms and DFT-calculated **b)** cumulative and **c)** differential pore size distributions of **NU-901-RT** before and after acid treatment and **Pt@NU-901**.

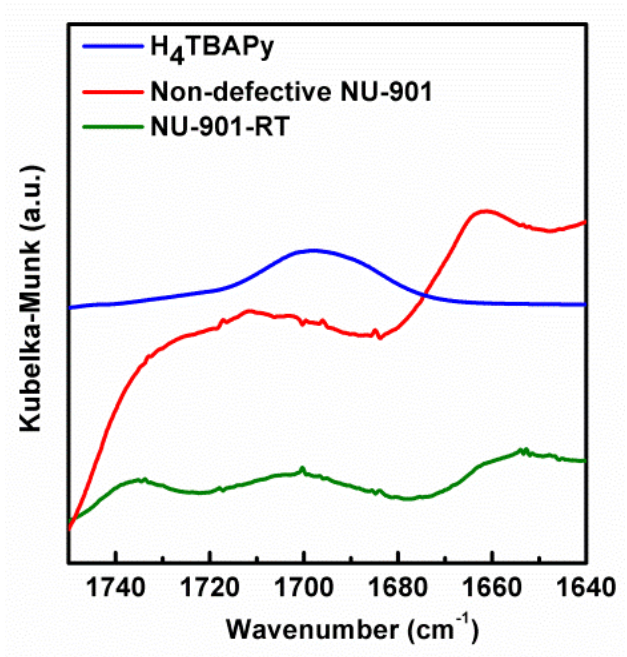

Figure S4. DRIFT spectra of **NU-901-RT**, Non-defective **NU-901**, and free H_4TBAPy linker. The MOF spectra are multiplied by a factor of 20 for clarity.

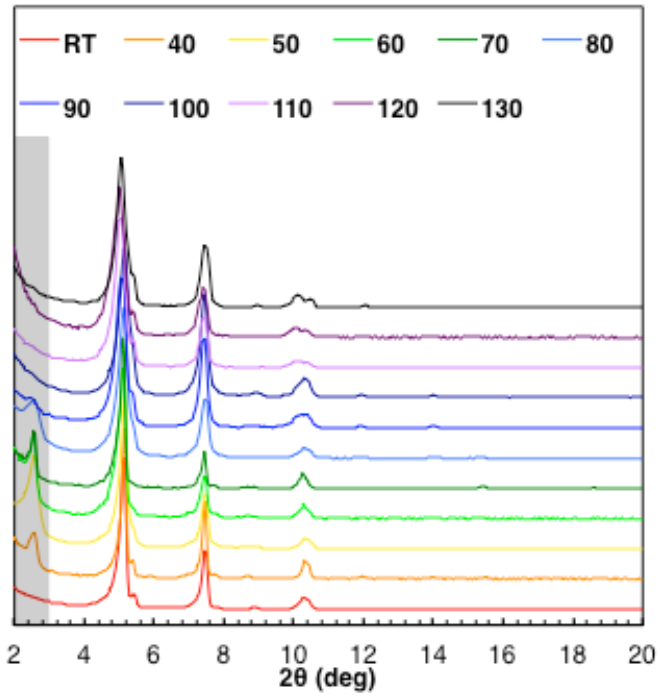

Figure S5. PXRD patterns of **NU-901** synthesized at various temperatures. The 2θ = 2.5° peak is highlighted in gray.

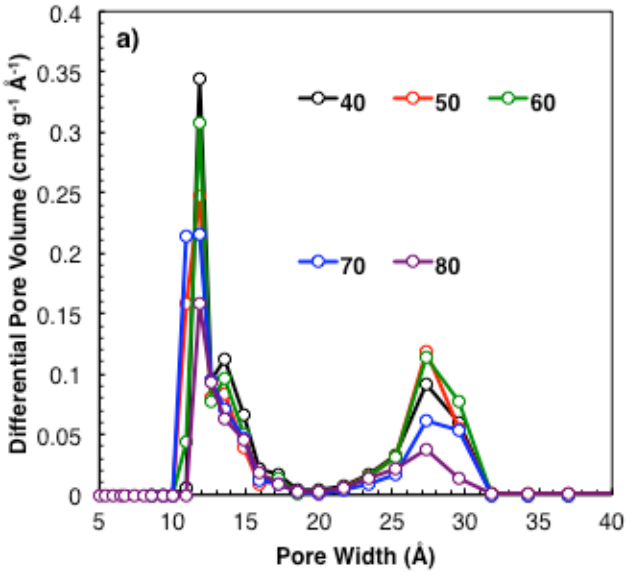

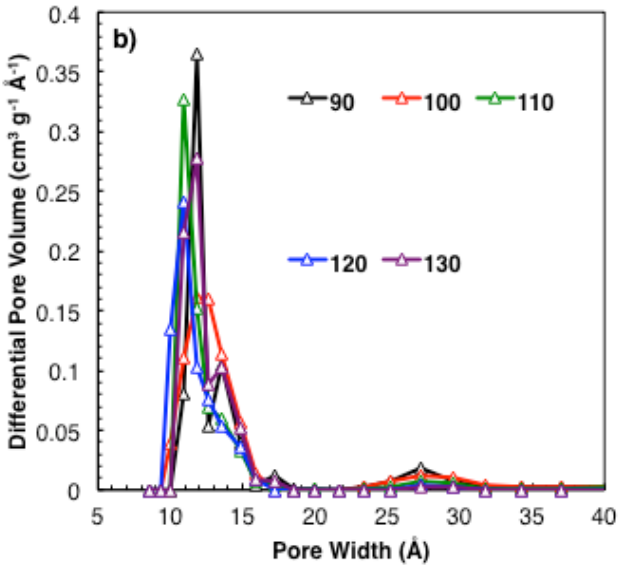

Figure S6. DFT-calculated pore size distribution of **NU-901** synthesized at various temperatures. For the N_2 isotherms, see **Figure 3**.

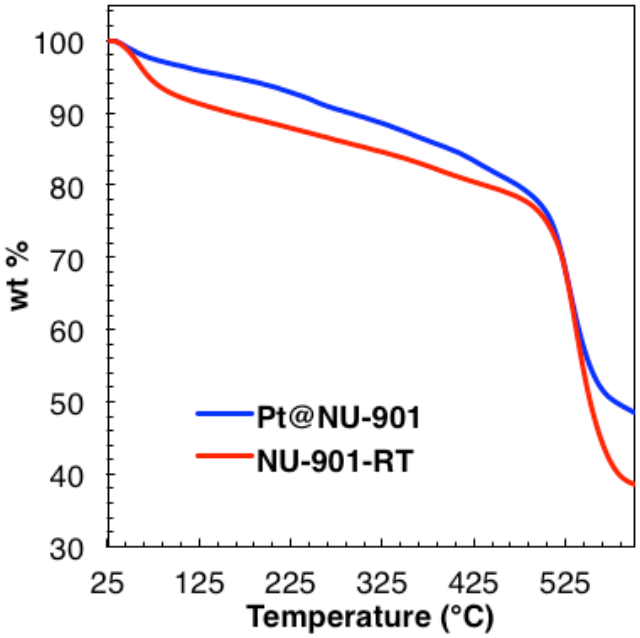

Figure S7. TGA traces of **NU-901-RT** and **Pt@NU-901**. The difference in wt % at 600 °C is 10 wt % similar to that determined through the ICP-OES measurements.

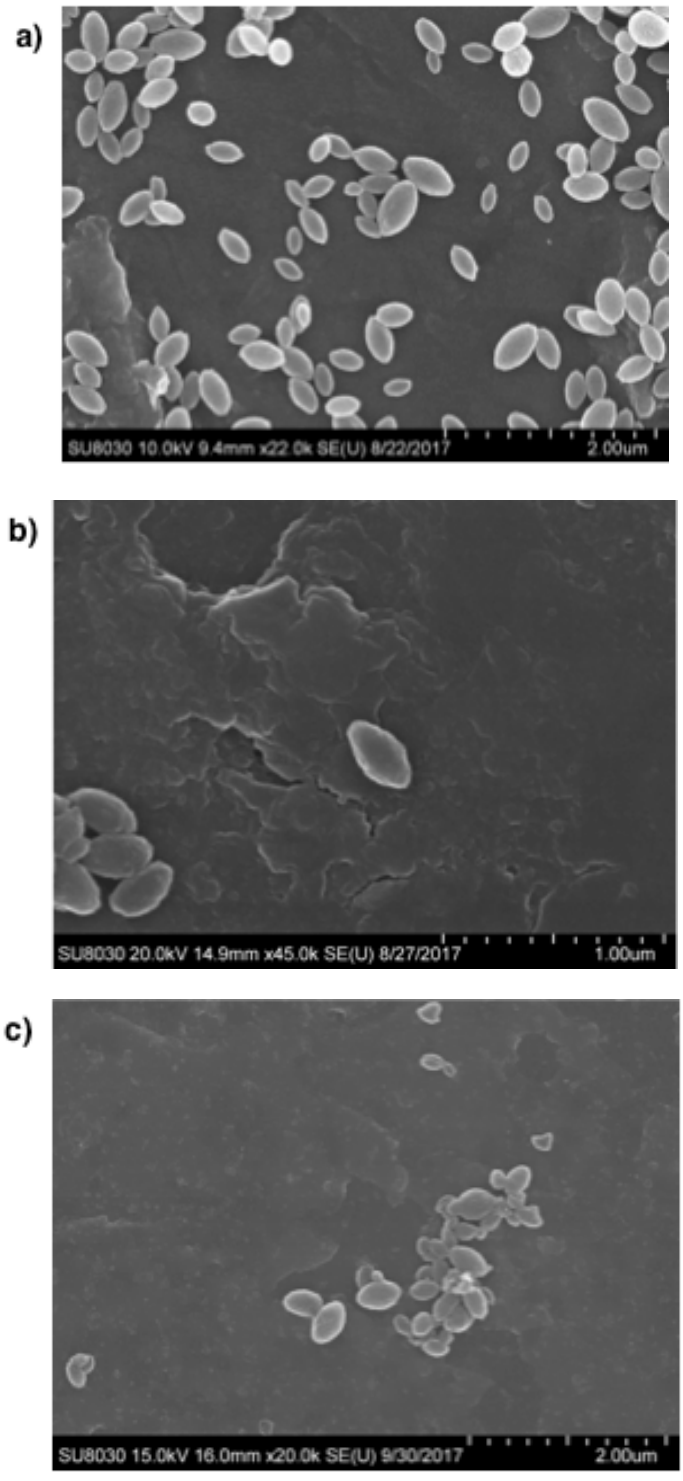

Figure S8. SEM images of **a) NU-901-RT** and **Pt@NU-901 b)** before and **c)** after catalysis.

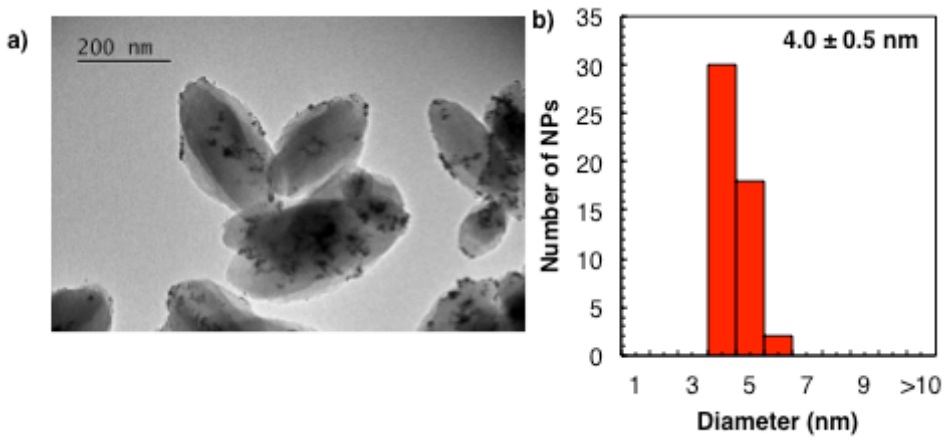

Figure S9. a) TEM image of **Pt@NU-901** and **b)** histogram for the particle size distribution of encapsulated Pt NPs.

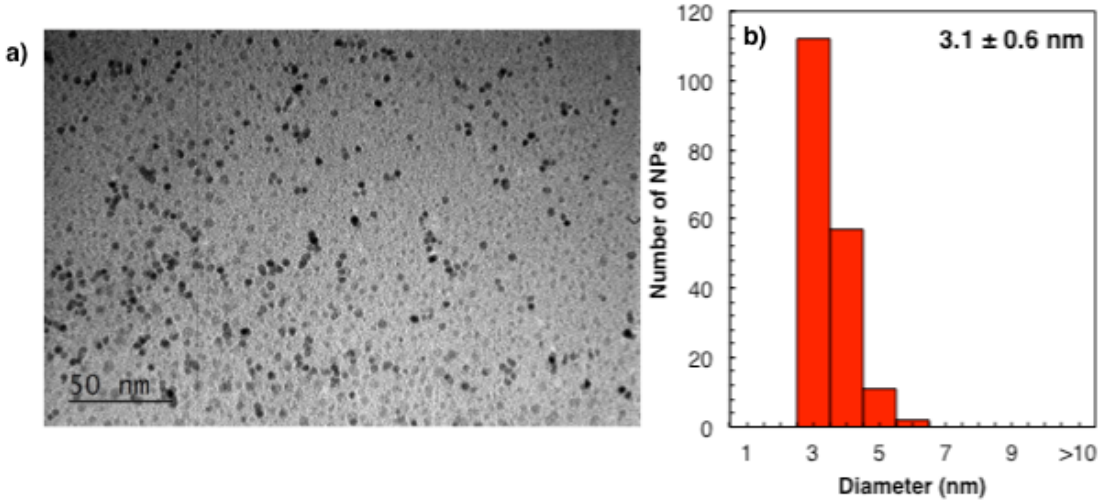

Figure S10. a) TEM image and **b)** size distribution of Pt NPs before encapsulation.

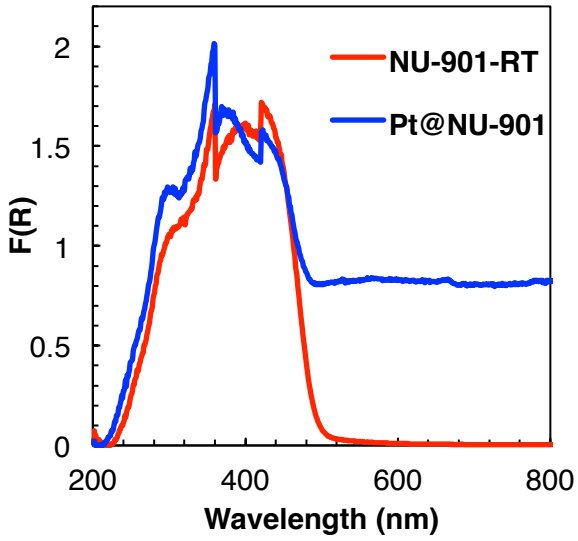

Figure S11. Diffuse reflectance UV-Vis Spectra of **NU-901-RT** and **Pt@NU-901**. Enhanced extinction in 500–800 nm region is attributed to the scattering due to close packing of Pt NPs and the MOF.

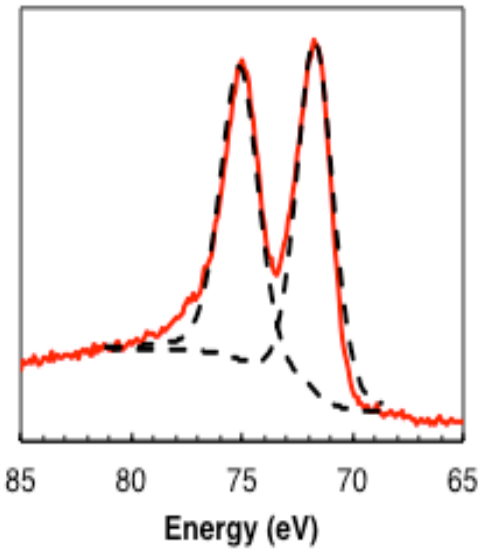

Figure S12. Pt 4f XPS spectrum of **Pt@NU-901**.

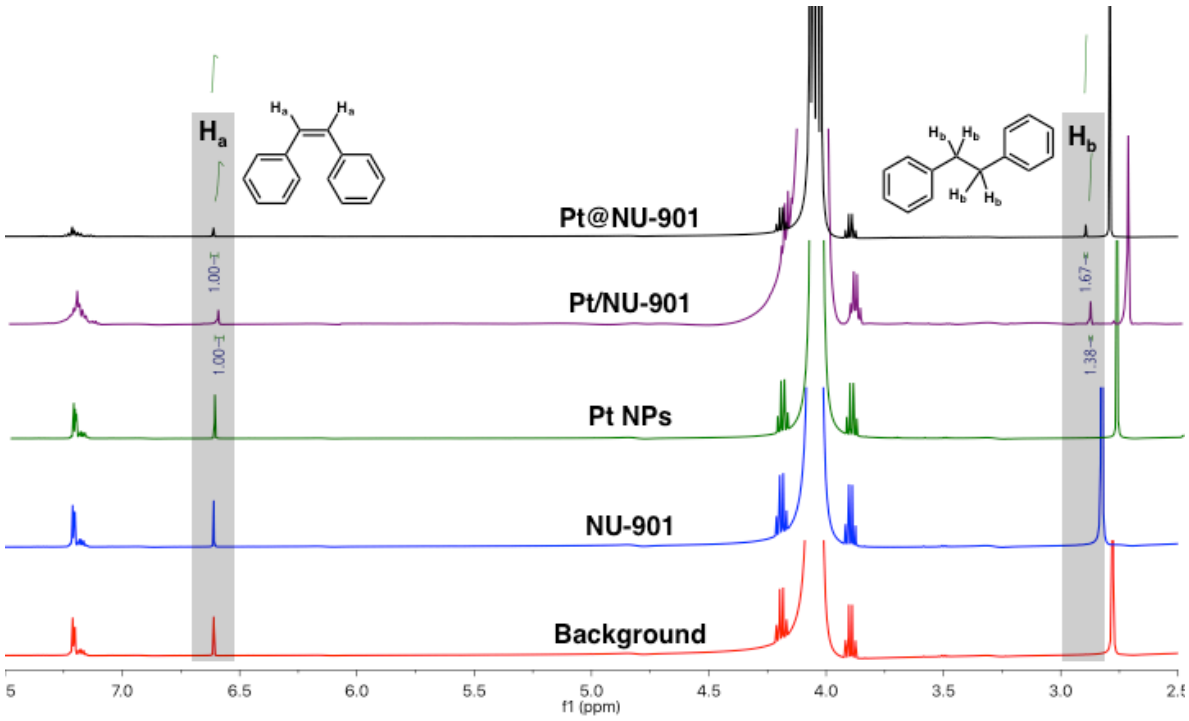

Figure S13. ^{1}H NMR spectra of all reaction mixtures after 1 h.

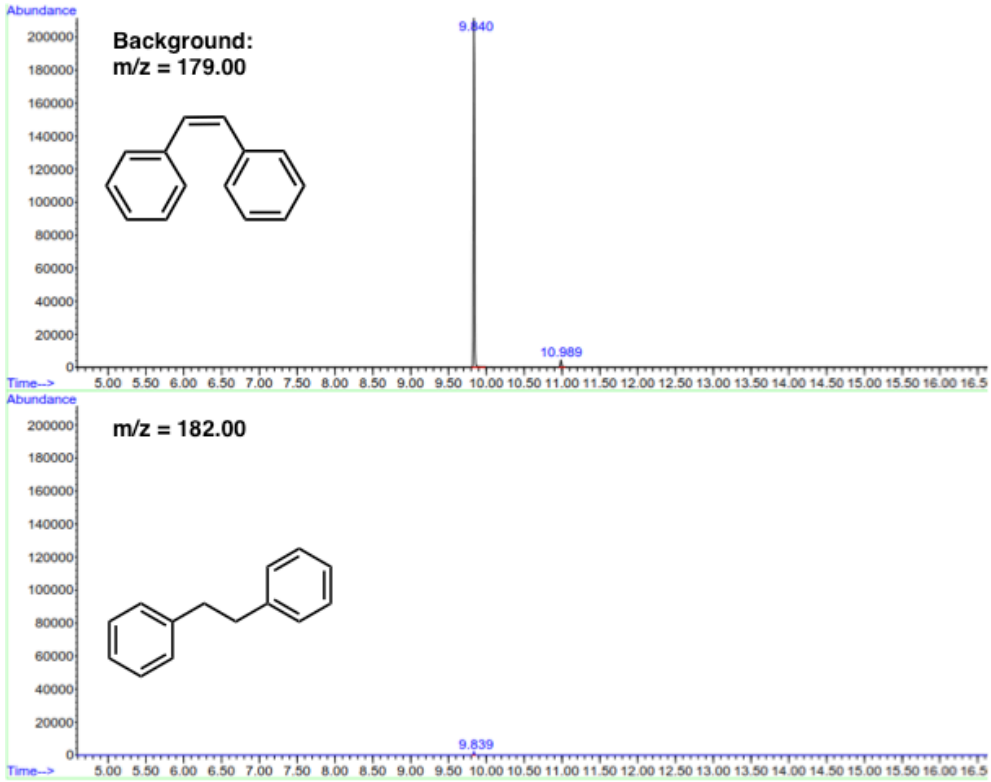

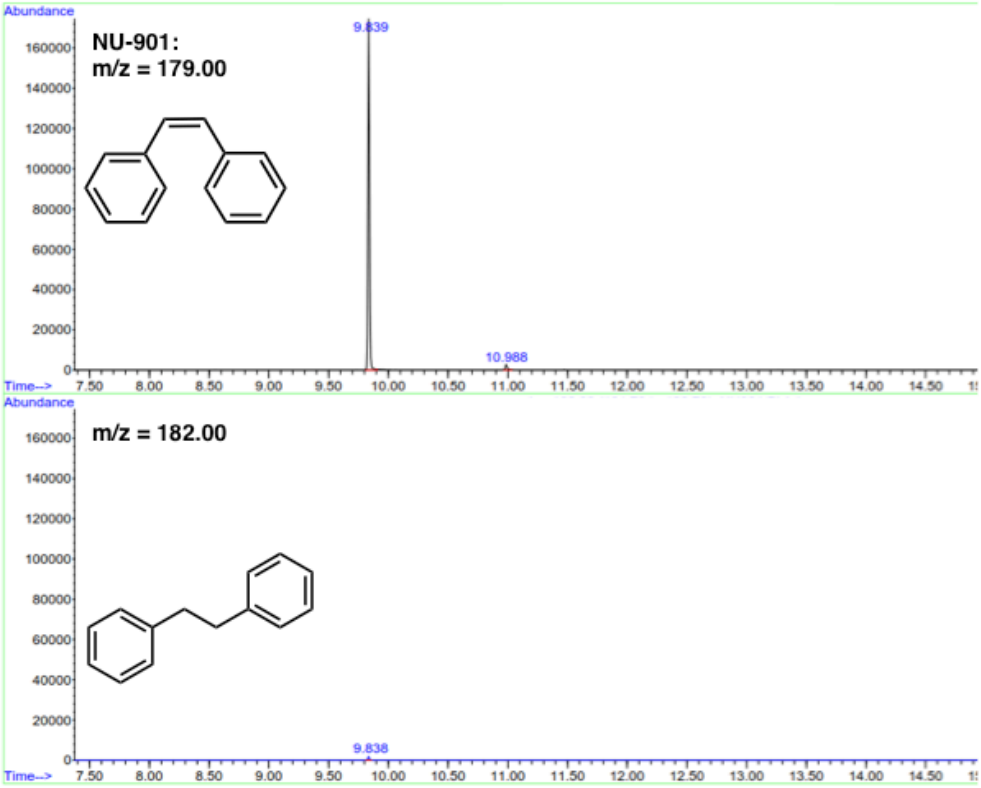
Abundance
NU-901:
m/z = 179.00
9.839
10.988
Time-->
m/z = 182.00
9.838

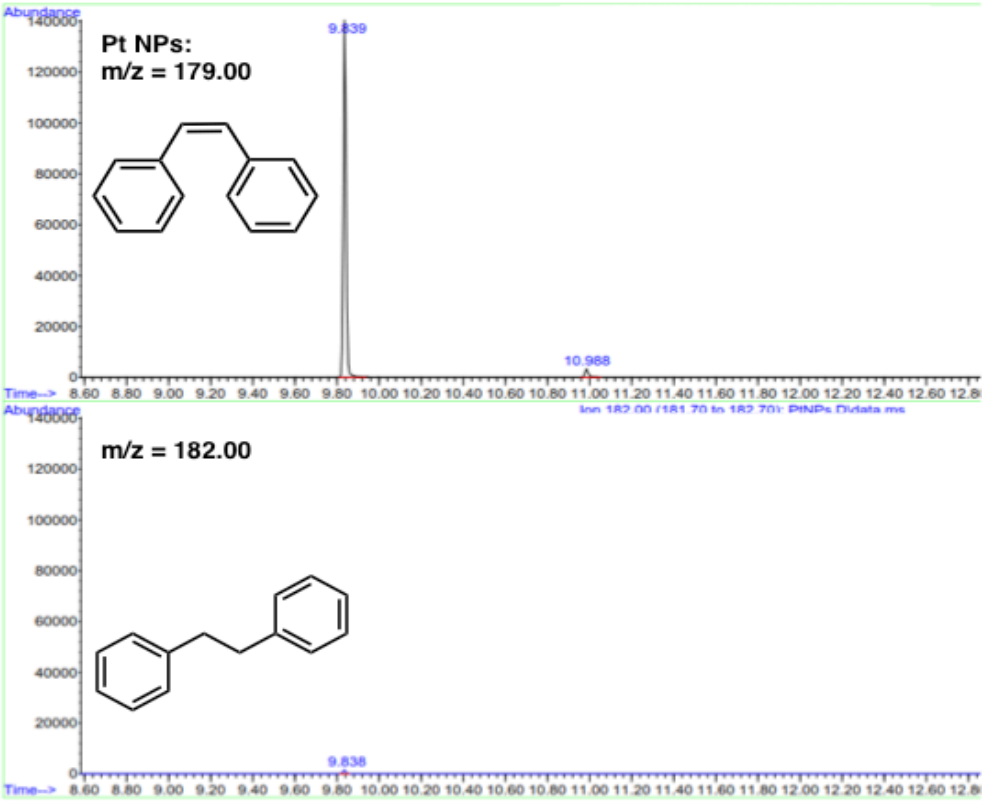
Abundance
Pt NPs:
m/z = 179.00
9.839
10.988
Time-->
m/z = 182.00
9.838

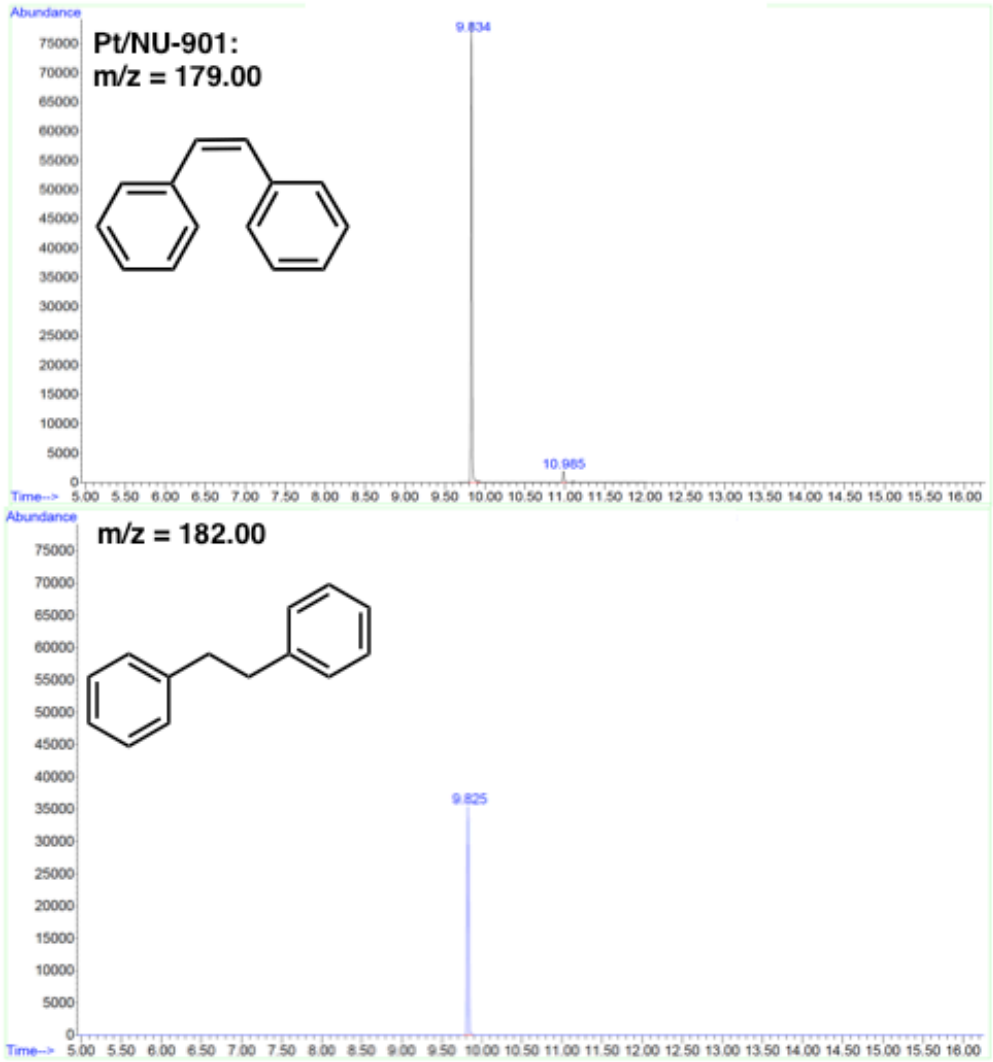
Abundance
Pt/NU-901:
m/z = 179.00
9.834
10.985
Time-->
m/z = 182.00
9.825

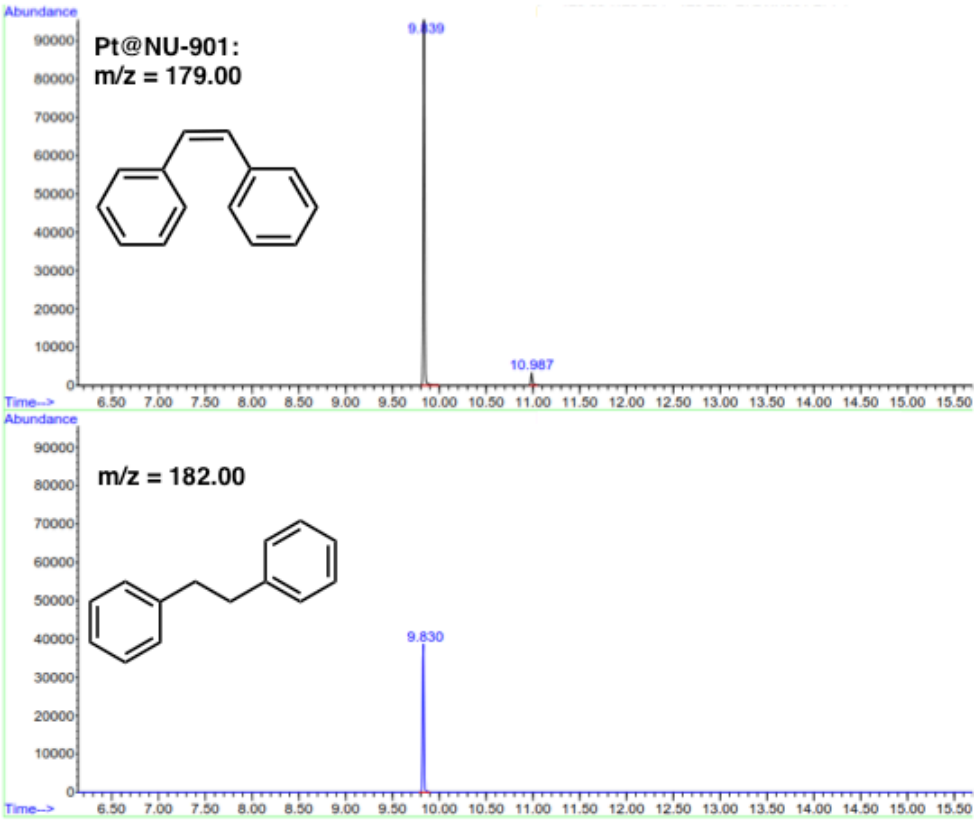
Abundance
Pt@NU-901:
m/z = 179.00
9.839
10.987
Time-->
m/z = 182.00
9.830

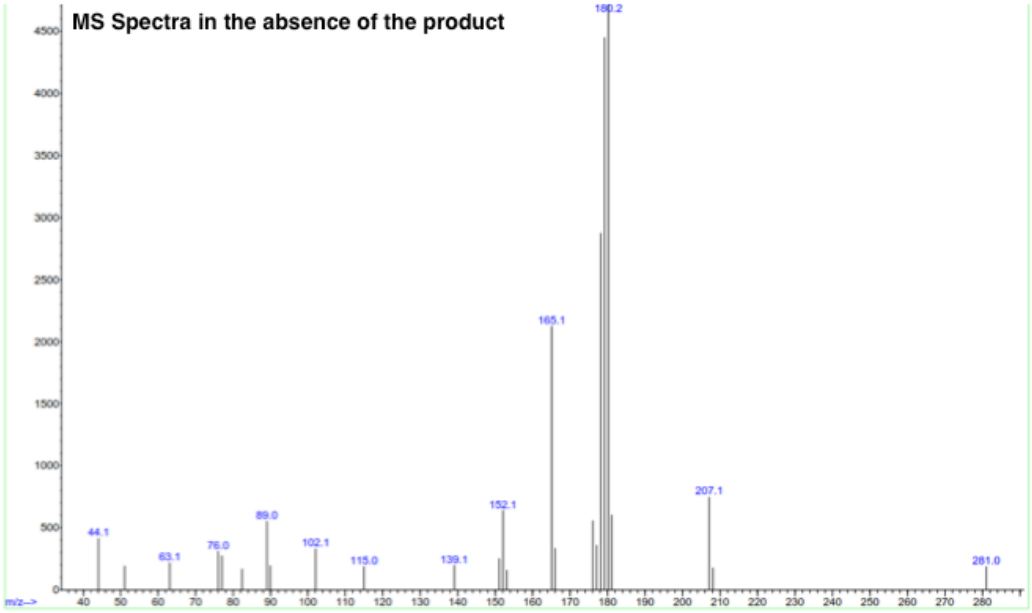
MS Spectra in the absence of the product
180.2
165.1
207.1
152.1
89.0
102.1
44.1
63.1
76.0
115.0
139.1
281.0
m/z-->

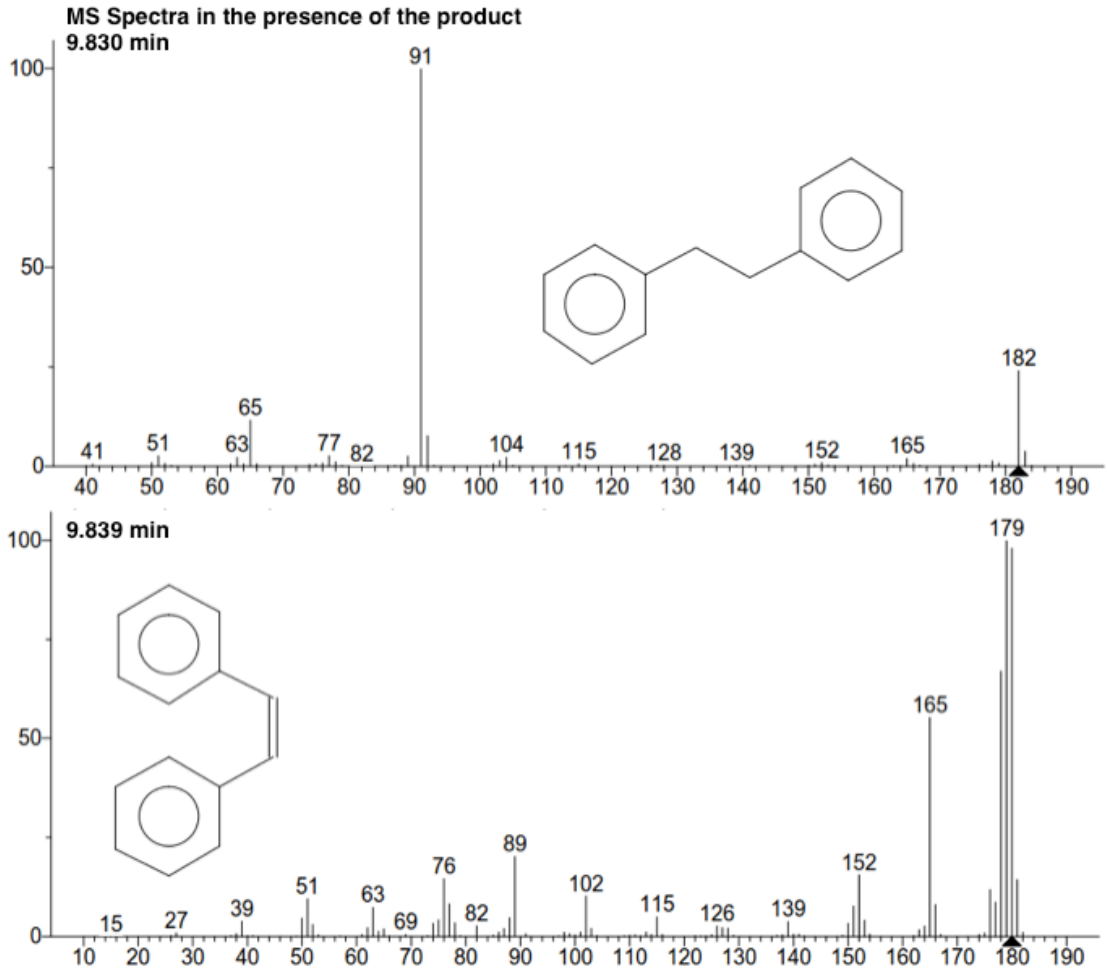

Figure S14. GC-MS spectra of all reaction mixtures after 1 h. The MS spectra of all controls showed no detectable amount of a molecule with m/z = 182, suggesting an absence of bibenzyl.

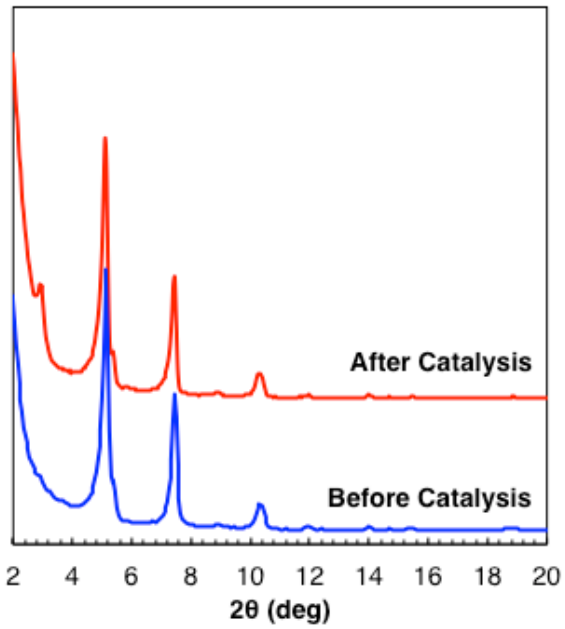

Figure S15. PXRD patterns of **Pt@NU-901** before and after *cis*-stilbene hydrogenation.

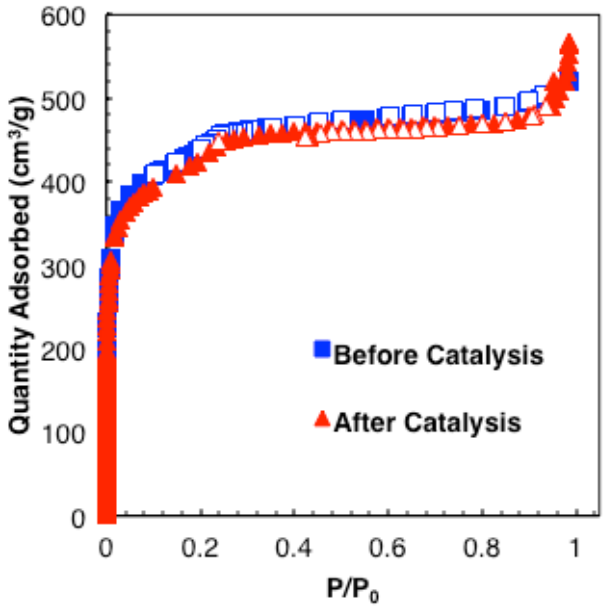

Figure S16. N_2 isotherm at 77 K of **Pt@NU-901** before and after catalysis.

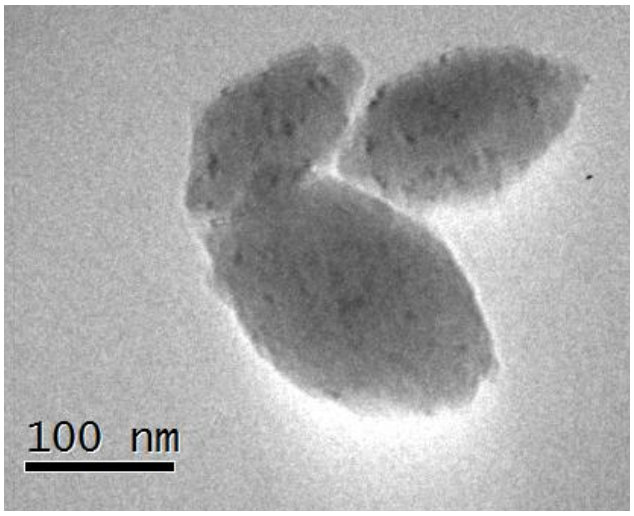

Figure S17. TEM image of **Pt@NU-901** after catalysis.

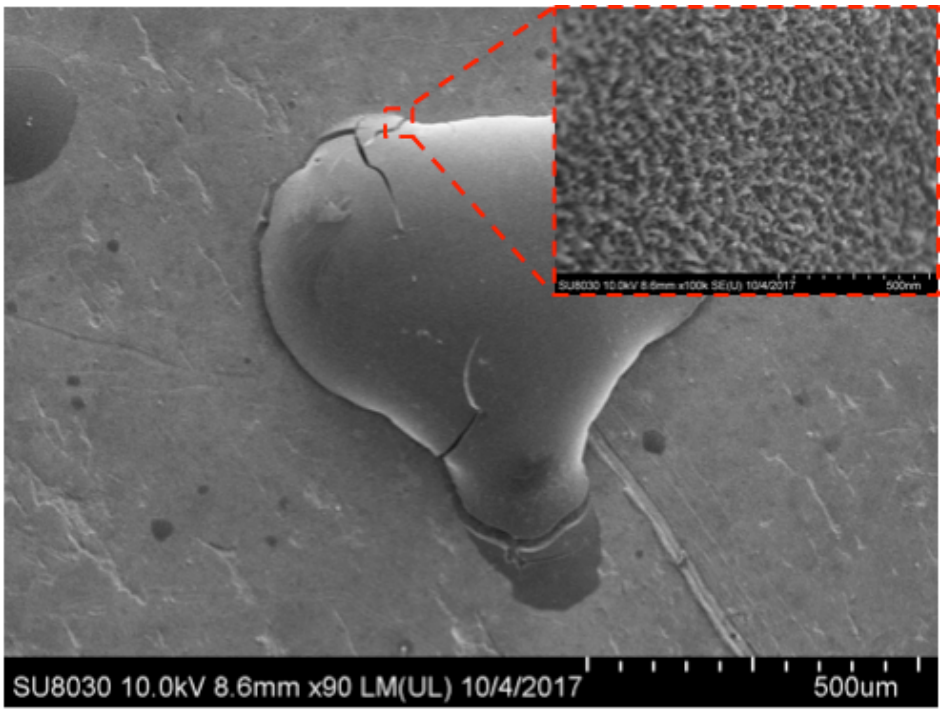

Figure S18. SEM images of bare Pt NPs after 1 h of catalysis.

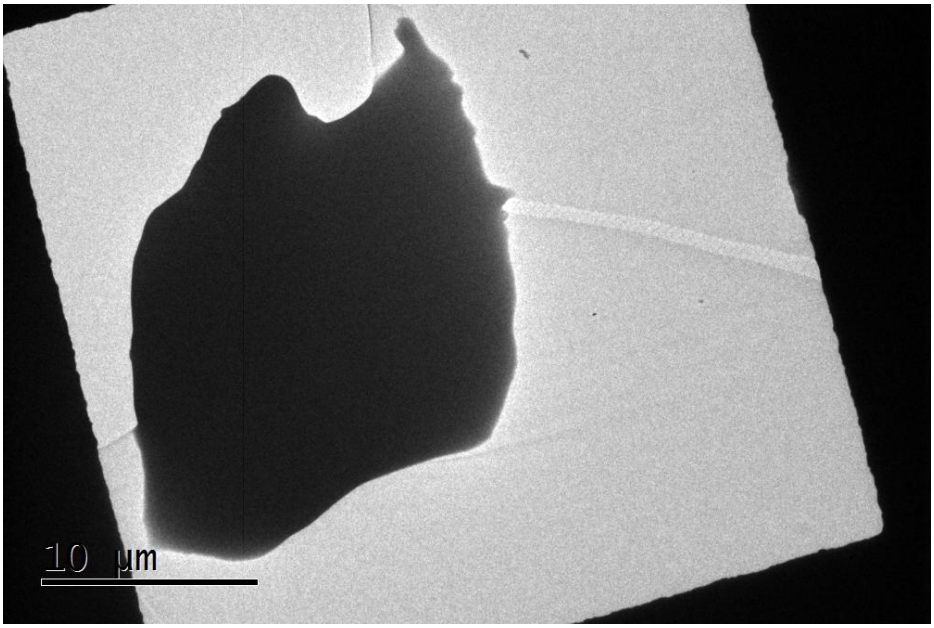

Figure S19. TEM image of bare Pt NPs after 1 h of catalysis.

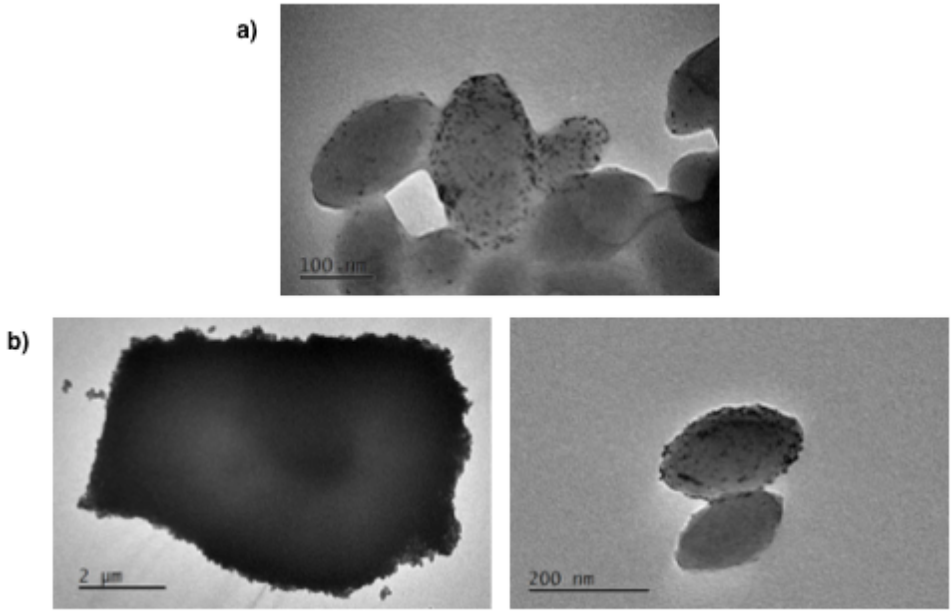

Figure S20. TEM images of **Pt/NU-901** (i.e. Pt NPs on the exterior surface of **NU-901**) **a)** before and **b)** after catalysis.

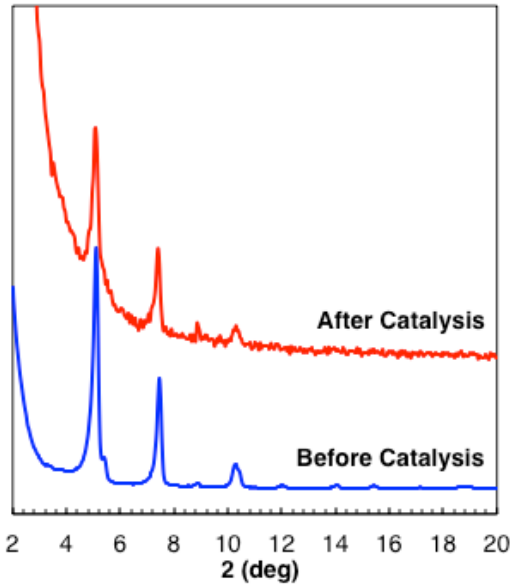

Figure S21. PXRD patterns of **Pt/NU-901** before and after *cis*-stilbene hydrogenation.

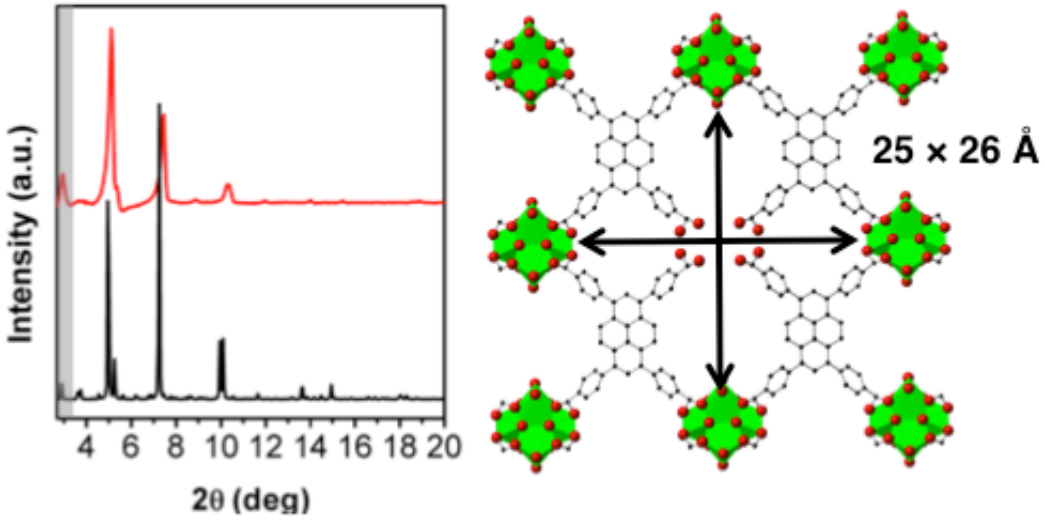

Figure S21. Simulated PXRD pattern of a missing Zr_6 node structure, as represented by the figure on the right (viewed from the *a*-axis of the crystal). Note the similar dimension of the mesopore as to that determined through the DFT-calculated pore size distribution.

References:

(1) Wang, T. C.; Vermeulen, N. A.; Kim, I. S.; Martinson, A. B. F.; Stoddart, J. F.; Hupp, J. T.; Farha, O. K., Scalable synthesis and post-modification of a mesoporous metal-organic framework called NU-1000, *Nat. Protocols* **2016,** *11*, 149-162.

(2) Howarth, A. J.; Peters, A. W.; Vermeulen, N. A.; Wang, T. C.; Hupp, J. T.; Farha, O. K., Best Practices for the Synthesis, Activation, and Characterization of Metal–Organic Frameworks, *Chem. Mater.* **2017,** *29*, 26-39.

(3) Kung, C.-W.; Wang, T. C.; Mondloch, J. E.; Fairen-Jimenez, D.; Gardner, D. M.; Bury, W.; Klingsporn, J. M.; Barnes, J. C.; Van Duyne, R.; Stoddart, J. F.; Wasielewski, M. R.; Farha, O. K.; Hupp, J. T., Metal–Organic Framework Thin Films Composed of Free-Standing Acicular Nanorods Exhibiting Reversible Electrochromism, *Chem. Mater.* **2013,** *25*, 5012-5017.

(4) Kickelbick, G.; Wiede, P.; Schubert, U., Variations in capping the Zr6O4(OH)4 cluster core: X-ray structure analyses of [Zr6(OH)4O4(OOC–CH=CH2)10]2(μ-OOC–CH=CH2)4 and Zr6(OH)4O4(OOCR)12(PrOH) (R = Ph, CMe = CH2), *Inorg. Chim. Acta* **1999,** *284*, 1-7.

(5) Stephenson, C. J.; Hupp, J. T.; Farha, O. K., Postassembly Transformation of a Catalytically Active Composite Material, Pt@ZIF-8, via Solvent-Assisted Linker Exchange, *Inorg. Chem.* **2016,** *55*, 1361-1363.